Proc. Natl. Acad. Sci. USA
Vol. 80, pp. 1501–1505, March 1983
Biochemistry

Model for mammalian metallothionein structure

(113Cd NMR/1H NMR/domains/metal)

YVAN BOULANGER, CHRISTOPHER M. GOODMAN, CARLA P. FORTE, STEPHEN W. FESIK, AND IAN M. ARMITAGE*

Department of Molecular Biophysics and Biochemistry, Yale University, New Haven, Connecticut 06510

Communicated by R. G. Shulman, December 2, 1982

ABSTRACT **The results of physicochemical studies of mammalian metallothioneins are summarized and used to propose a model of the protein. The primary structures of all mammalian metallothioneins are very homologous; there are 38 invariant residues and 20 of them are cysteines. The results of UV and CD optical studies indicated that all 20 cysteines are involved in the ligation of 7 mol of metal per mol of metallothionein and that the protein does not contain any α-helix structure. A theoretical analysis by the Chou–Fasman method has predicted 11 β-bends, each one involving at least one cysteine residue. The most significant structural data, provided by ^{113}Cd NMR, demonstrated that the 7 mol of bound Cd^{2+} are arranged in two separate metal clusters, one containing four metal ions and the other containing three, with all Cd^{2+} tetrahedrally coordinated to cysteine thiolate ligands. The 11 cysteine residues of the carboxyl-terminal portion of the metallothionein chain (residues 30–61) are ligated to the 4-metal cluster as shown by ^{113}Cd NMR of this enzymatically cleaved fragment. The remaining cysteine residues from the amino-terminal polypeptide portion (residues 1–29) form the 3-metal cluster. Such a division of the chain is consistent with the presence of an intron in the mouse metallothionein-1 gene corresponding to residue 32 in the polypeptide chain. A two-domain molecular model has been constructed based on an analysis of all the available data and is described in detail. The accuracy of this model was tested by ^{1}H NMR at 500 MHz and the data are in agreement with our proposed structure.**

Metallothioneins (MTs) comprise a class of low molecular weight, cysteine-rich metal binding proteins, the first of which was isolated from equine renal cortex (1). Since then, various investigators have characterized similar proteins from kidney and liver tissue of other mammals, as well as in birds, fish, crustaceans, and even microorganisms (2). Through thiolate bonds, the protein sequesters various metallic cations such as cadmium, zinc, copper, and mercury (3), and its biosynthesis is closely regulated by the level of exposure of an organism to salts of these metals (4). The metal composition depends on the species, the tissue, the stage of development, and the exposure of the organism to metals (4–6). It is these characteristic properties of MT that are responsible for the proposal that this protein plays an important, as yet undefined, function in the metabolism or homeostasis of essential heavy metals (7, 8) as well as functioning as a detoxifying agent by sequestering toxic metals (9). In most cases, the protein exists in two major isoprotein forms, MT-1 and MT-2, which differ in amino acid composition and in total charge. These two isoprotein forms are usually present in comparable amounts; however, their ratio has been reported to be affected by metal induction (10).

As a consequence of unsuccessful efforts in our own laboratory and others to crystallize MT, a detailed x-ray crystal structure is not available. However, extensive ^{113}Cd NMR studies from this laboratory (11–15) have revealed that the 7 mol of Cd^{2+} bound per mol of mammalian MT are located in two separate metal clusters, one containing four Cd^{2+} (cluster A) and the other containing three (cluster B). Furthermore, these studies have shown that the two clusters exhibit significant differences in their affinity for different metal ions (e.g., Cd^{2+}, Zn^{2+}, and Cu^{+}) and that they function independently of one another.

When these data are analyzed in conjunction with other physicochemical data for this protein, including extensive amino acid sequence homologies for MTs from different species (16–25), UV and CD spectral properties (26–29), and gene structure (30–32), there emerges a self-consistent two-domain model for the tertiary structure of this protein. Strong evidence in support of this model was recently obtained from ^{113}Cd NMR studies on a fragment of MT obtained by enzymatic degradation and shown to contain four metals (33, 34).

The present article briefly reviews previous structural data on this protein and describes the incorporation of these and new data into a model of the tertiary structure for this protein. Confirmation of several features in the predicted structure is provided by high-field ^{1}H NMR data and is discussed in detail.

Amino acid sequence

The amino acid sequences of MTs from several mammalian sources have been determined (16–23) and all were found to possess a 61-amino acid chain of remarkably similar composition. All contain 20 cysteine residues whose positions are invariant along the chain. Ten of the cysteines are found in five Cys-X-Cys units, where X is a variable residue. Seven more of the cysteines are present in two groups, Cys-Cys-X-Cys-Cys (positions 33–37) and Cys-X-Cys-Cys (positions 57–60). All the cysteines are known to be involved in the coordination of 6–7 molecules of metal per molecule of MT (3) and the repetitive locations of these patterns suggest a common metal coordination mode for all mammalian MTs. In addition, 18 other residues are common to all sequences known to date. The primary structure of MT is also notable for its high content of lysine (6–8 residues) and serine (7–10 residues) and for its total lack of aromatic and histidine residues.

Physicochemical properties

The general shape of the protein, calculated from its hydrodynamic properties during gel filtration (35), has been represented as a prolate ellipsoid with an axial ratio a/b of 6. The protein has also been studied by using dark-field electron microscopy and shown to have an elongated shape with dimensions 36 × 25

The publication costs of this article were defrayed in part by page charge payment. This article must therefore be hereby marked "*advertisement*" in accordance with 18 U. S. C. §1734 solely to indicate this fact.

Abbreviations: MT-1 and MT-2, metallothionein-1 and -2; NOE, nuclear Overhauser enhancement.

* To whom reprint requests should be addressed.

× 16 Å (36). Both methods indicate that MT has a nonspherical shape although the absolute dimensions differ significantly, possibly because the molecule adopts different conformations in different media or because of the experimental uncertainties associated with these methods.

The CD and UV spectra of MT have been recorded for the Cd^{2+}, Zn^{2+}, and Cu^{+} forms of the protein (26–29). Broad UV and CD absorption bands, characteristic of the metal–thiolate charge transfer transitions, were observed in each case. Unfortunately, due to the overlapping metal–thiolate charge transfer transitions, neither the UV nor the CD spectrum allows a detailed structural characterization of the individual metal-binding sites although recent spectral simulations are suggestive of tetrahedral metal–thiolate coordination (29).

Analysis of the shape of the CD ellipticity bands showed that little or no secondary structure, such as α-helix or β-pleated sheet, was present in the polypeptide chain, whether or not it contained metals. In both cases the observed spectra are similar to those obtained from random coil polypeptides and denatured proteins. Whereas this technique is particularly sensitive to the α-helix structure, it is important to note that no unequivocal conclusions can be derived from these measurements regarding the extent of the β-structure due to the inherent limitations of this technique (37).

Chou–Fasman predictions

The results from the application of the Chou–Fasman method for secondary structure predictions (38) in the human MT-2 sequence are given in Table 1. Although these calculations predict short regions of α-helix and β-sheet, by far the dominant structural feature predicted by this method is the 11 β-bends, 10 with a high probability. These predictions are in complete agreement with the elements of the secondary structure that can be obtained from an analysis of the CD bands. Thus, in the absence of metals, the protein is predicted to form an exceptionally large number of β-bends, each containing one or two cysteine residues, which generates a secondary structure ideally poised for the binding of the multiple metal ions, as will be apparent later.

^{113}Cd NMR studies

A detailed elucidation of the structure of the individual metal coordination sites was obtained from the ^{113}Cd NMR studies of the isotopically labeled ^{113}Cd–MT isolated from rabbit, calf, and human livers (11–15). In all cases, several multiplets were observed in the chemical shift range of 600–670 ppm, consistent with tetrahedral sulfur coordination to cysteine residues (39). A detailed analysis of the observed ^{113}Cd–^{113}Cd scalar couplings by homonuclear decoupling and two-dimensional techniques showed that the seven atoms of bound Cd^{2+} in all mammalian MTs are arranged in two separate clusters, one containing three and the other four metal ions with the proposed structure as shown in Fig. 1A. The 3-metal cluster forms a cyclohexane-like six-membered ring requiring 9 cysteine thiolate ligands whereas the 4-metal cluster forms a bicyclo [3:1:3] structure, requiring 11 cysteine thiolate ligands. In total, five metal ions are linked to two bridging and two nonbridging cysteines, and two metal ions are linked to three bridging and one nonbridging cysteine.

In some cases, two multiplets are observed for a particular ^{113}Cd resonance; these have been attributed to a mixture of two or more proteins with limited heterogeneity in the primary structure (12, 14). For example, the ^{113}Cd spectrum of human liver ^{113}Cd–MT-2 shows no sign of resonance duplication whereas that of human liver MT-1 shows heterogeneity both in the 3-metal cluster ^{113}Cd resonances and at resonance 5 which has been assigned to the 4-metal cluster. The primary structure of human MT-2 is homogeneous, whereas MT-1 is a mixture of at least two proteins with primary structure heterogeneity in six different positions (32). Both isoproteins from rabbit liver are a mixture of at least two proteins, and resonance duplication is observed in all four of the ^{113}Cd resonances assigned to the 4-metal cluster (12).

The absence of resonances assigned to the 3-metal cluster in the spectrum of calf liver ^{113}Cd, Cu-MT-1 (13), reflects the preference of Cu^{+} for the 3-metal cluster. In the case of the rabbit liver ^{113}Cd,Zn–MT hybrid, analysis of the ^{113}Cd spectrum showed that the Zn^{2+} was bound preferentially (>85%) to the 3-metal cluster. Thus, the ^{113}Cd NMR studies have revealed significant differences in the affinity of the two clusters for different metal ions. For the 3-metal cluster, the affinity is found to decrease in the order $Cu^{+} > Zn^{2+} > Cd^{2+}$. Exactly the reverse order applies to the 4-metal cluster.

In a recent study, rat liver MT was enzymatically digested and a polypeptide fragment containing 11 cysteine residues and 4 bound Cd^{2+} was isolated (33). The amino acid composition of this fragment, designated α_I, corresponds to residues 30–61 of the rat MT sequence. The ^{113}Cd NMR spectrum from the Cd-α_I MT-1 fragment shows four resonances with the chemical shifts corresponding to the resonances assigned to the 4-metal cluster in the intact protein (34). This result provides unequivocal evidence for the existence of two separate domains in the MT structure.

Table 1. Chou–Fasman predictions of the secondary structure for human MT-2

	1 Met	Asp	Pro	Asn	Cys	Ser	Cys	Ala	Ala	10 Gly	Asp	Ser	Cys	Thr	Cys	Ala	Gly	Ser	Cys	20 Lys	Cys	Lys	Glu	Cys	Lys
α-Helix*	0	0	0	0	0	0	0	0	0	0	0	0	0	0	0	0	0	0	0	7	8	8	8	8	6
β-Sheet*	0	0	0	0	0	0	0	0	0	0	0	7	8	8	6	0	0	0	0	0	0	0	0	7	8
β-Bends†	0	2	2	2	2	0	0	0	0	0	2	2	2	2	2	2	2	2	2	2	2	2	0	0	0
	Cys	Thr	Ser	Cys	30 Lys	Lys	Ser	Cys	Cys	Ser	Cys	Cys	Pro	Val	40 Gly	Cys	Ala	Lys	Cys	Ala	Gln	Gly	Cys	Ile	50 Cys
	0	0	0	0	0	0	0	0	0	0	0	0	0	0	0	7	8	8	8	8	6	0	0	0	0
	8	6	0	0	0	0	0	7	8	8	8	6	0	0	0	0	0	0	0	5	7	8	8	8	6
	2	2	2	2	0	2	2	2	2	0	0	2	2	2	2	1	1	1	1	2	2	2	2	0	2
	Lys	Gly	Ala	Ser	Asp	Lys	Cys	Cys	Ser	60 Cys	Ala														
	0	0	0	0	0	0	0	0	0	0	0														
	0	0	0	0	0	0	7	8	8	6	0														
	2	2	2	0	2	2	2	2	0	0	0														

* 5, Probable NH_2-terminal extension; 7, definite start to NH_2 terminus; 8, central region prediction; 6, definite COOH terminus end; 4, probable COOH-terminal extension.

† 1, Possible bend; 2, probable bend.

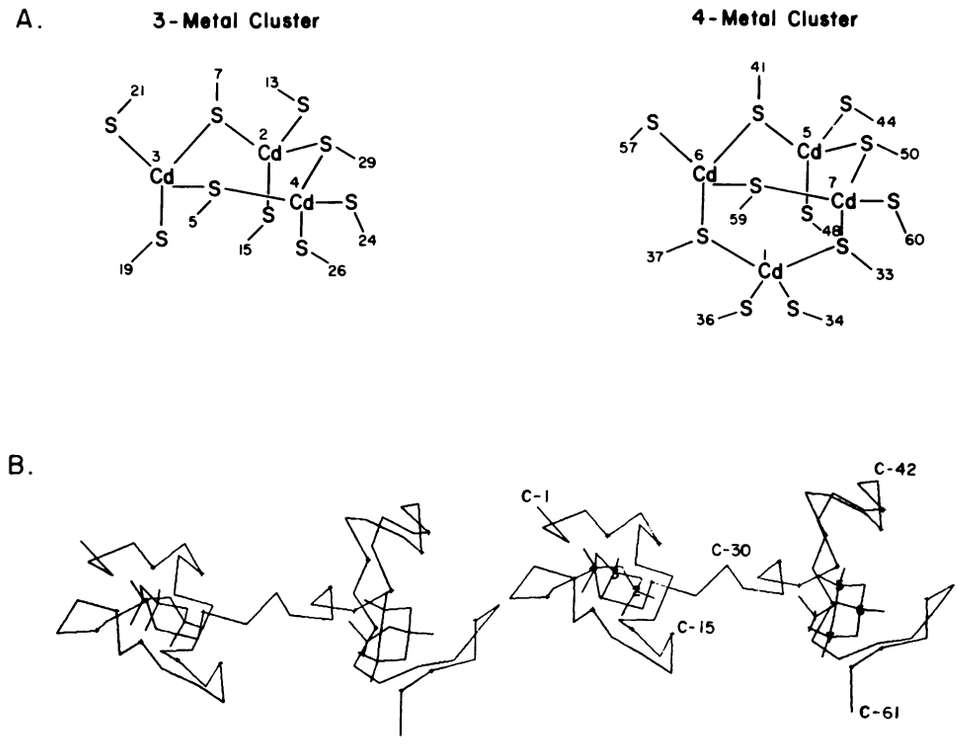

FIG. 1. (*A*) Structures of the 3-metal and 4-metal clusters in mammalian MTs based on ^{113}Cd NMR data and other considerations discussed in the text. The Cd numbering corresponds to the respective ^{113}Cd NMR multiplets (12) and the S numbering indicates the arrangement of the cysteine residues in the model. (*B*) Stereo computer graphics of the proposed model of mammalian MT showing the α carbons of the peptide chain and the detached metal clusters. The metal ions are labeled with their respective numbers.

Regulation and gene structure

In view of the recent assertion of a correspondence between the intron/exon structure of eukaryotic genes and the domains of proteins (40), it is interesting to consider the structure of the mouse MT-1 (30, 31) and human MT-2 (32) genes determined by heteroduplex mapping and by sequence analysis. These studies showed that the chain is divided into three exons corresponding to amino acid residues 1–9, 10–31, and 32–61, respectively. Division of the chain after the second exon would give a portion containing 9 cysteines (positions 1–31) and a portion containing 11 cysteines (positions 32–61) which would correspond to the proposed structure of the 3- and 4-metal cluster, respectively. Of particular interest is the correspondence observed between the polypeptide structure encoded by one of the exons and the polypeptide fragment obtained by limited proteolysis with subtilisin which gives a 32-residue polypeptide (corresponding to residues 30–61 in the amino acid sequence) that contained 4 bound Cd^{2+} ions (33).

Model building

Based on the structural and physicochemical data described above, a molecular model of MT has been constructed (Fig. 1*B*). The protein is constructed with two domains, one containing the 3- and the other the 4-metal cluster, corresponding to the NH_2-terminal and the COOH-terminal portions of the protein, respectively. The metal clusters consist of tetrahedral metal centers bound and bridged by cysteine sulfurs, as evidenced by ^{113}Cd NMR (11–15). The positions of the cysteines bound to the Cd metals are given in Fig. 1*A*. The 11 β-bends predicted by the Chou-Fasman calculations are also included in this model.

Whereas it is not possible to determine a unique distribution of the cysteine residues among the individual metal binding sites, the results from the genetic studies (30, 31), the subtilisin digestion (33, 34), and, when present, the heterogeneity from multiple isoproteins allowed us to divide the chain into two fragments, forming the 3-metal cluster (residues 1–30) and the 4-metal cluster (residues 31–61). The 3-metal cluster fragment contains four Cys-X-Cys groups (specifically, residues 5–7, 13–15, 19–21, and 24–26) and one isolated cysteine (residue 29). In deploying these cysteine residues in the cluster, we have assumed that each Cys-X-Cys group binds to the same metal, considering the short distance between the cysteines. Five β-bends, and associated H bonds, predicted by the Chou–Fasman program can also be easily built into this region.

Examination of the polypeptide fragment 31–61 of the chain shows three cysteine groups: the Cys-Cys-X-Cys-Cys group in positions 33–37, the Cys-X-Cys-Cys group in positions 57–60, and four cysteines in positions 41–50. With the assumption that adjacent cysteines participate in the coordination of the same metal, these same three cysteine groups can be retained in the proposed structure for the 4-metal cluster coordination as shown in Fig. 1*A*. In this structure, the cysteine residues in positions 33–37 and 41–50 participate as ligands to Cd_1 and Cd_5, respectively, and the cysteine residues in positions 57–60 participate as ligands to Cd_6 and Cd_7. The bridging cysteines (residues 33, 37, 41, and 50) are also linked to a second metal ion to form the cluster shown in Fig. 1*A*. Although the structure is symmetrical as drawn, this is almost certainly not the case in the protein as evidenced by the differences in the ^{113}Cd chemical shifts and coupling constants for this cluster (12). The six β-bends, and associated H bonds, predicted from the Chou–Fasman calculations are readily accommodated in this structural domain. It is interesting to note that, in this proposed structure, the polypeptide chain is tightly wrapped around the 4-metal cluster, which may explain the greater stability of the metals in this cluster in comparison to those in the 3-metal cluster.

Other structural contributions are provided by electrostatic interactions and H bonding involving side-chain residues (serine, threonine), for example, with the amide carboxyl of the peptide chain (O—H···O=C) (41). In Fig. 1*B*, all negatively charged residues (aspartate, glutamate, and the terminal alanine) have been coupled to positively charged residues (lysine, arginine). The two lysine residues in positions 30 and 31, at the junction between the two clusters, may participate in neutralizing the negative charge of the clusters and, in so doing, exert a structural role by bringing the two clusters closer together through

salt bridges. An interaction such as this would account for the absence of reactivity of the fully metalated MT with subtilisin (33).

Close examination of our proposed three-dimensional structure (Fig. 1*B*) reveals additional structural properties that offer reasonable explanations for other observations made in the ^{113}Cd NMR spectra. One such observation is the presence of two resonances for Cd_5 in the ^{113}Cd spectrum of human MT-1 (14). In our structure, the variable residue number 55 in this sequence, aspartate or glutamate, is located in close proximity to Cd_5. The negatively charged side chain of either of these residues could induce substantial differences in the electronic environment of Cd_5 which could account for the observation of two distinct Cd_5 resonances.

^1H NMR

Additional support for our model of the tertiary structure of MT has been obtained from ^1H NMR studies. Fig. 2 depicts the downfield region of the ^1H NMR spectra of intact rabbit MT and of the α_{II} fragment (rat) at 50°C in 95% H_2O. Approximately 11–13 well-resolved ^1H resonances were observed in the 6.5- to 9.5-ppm region of the spectrum of the intact protein (Fig. 2*A*), in agreement with a previous report (41). These resonances correspond to the slowly exchanging amide protons of MT which may be either shielded from the solvent or involved in a H bond. In support of the latter explanation is the correspondence between the number of slowly exchanging amide protons observed experimentally and the number of H-bonded protons involved in the 11 β-bends predicted from the Chou–Fasman calculations. For the α fragment, the Chou–Fasman calculations predict six β-bends. In the ^1H NMR spectrum of the α fragment (Fig. 2*B*), six slowly exchanging amide resonances were observed.

In comparison to the intact MTs, the ^1H NMR spectrum from the α fragment is much simpler and many of the ^1H resonances could be assigned on the basis of their chemical shifts and scalar connectivities. To aid in the total ^1H NMR assignments of the MT fragment, two-dimensional NMR methods (2D J-resolved,

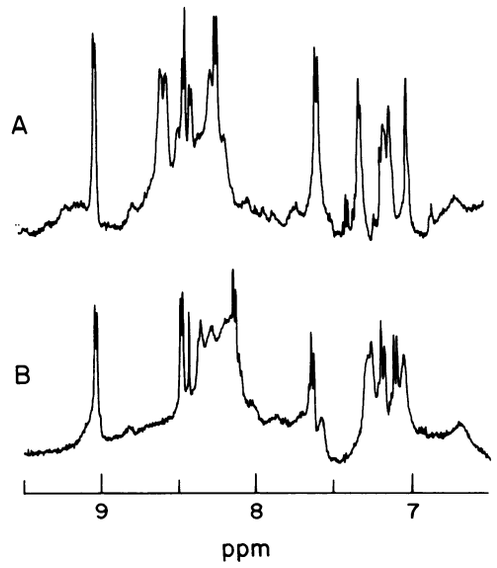

FIG. 2. ^1H NMR spectra (500 MHz). (*A*) Rabbit liver MT-1 (at 3 mM). (*B*) Rat liver α_{II} fragment (at 4 mM). Both spectra were acquired in 95% H_2O at 50°C by using the Redfield pulse sequence (2-1-4-1-2).

SECSY) and ^1H–^1H nuclear Overhauser enhancement (NOE) difference experiments were used at high magnetic fields (11.7 T) (unpublished data). The interpretations of the ^1H NMR data were greatly facilitated by the fact that several of the amino acid residues (aspartate, proline, valine, and isoleucine) of the fragment are unique (33)†. In addition to aiding in the assignments of the individual resonances, the NOE data provided new evidence in support of the tertiary structure of our model. When

† The amino acid composition of the α_{II}-MT fragment used in this study was previously reported by Winge and Miklossy (33). Our analysis of the ^1H NMR spectra and redetermination of the amino acid composition indicates the following corrections: two glutamines (or glutamic acids) and one isoleucine as opposed to the reported three glutamines (or glutamic acids) and no isoleucine.

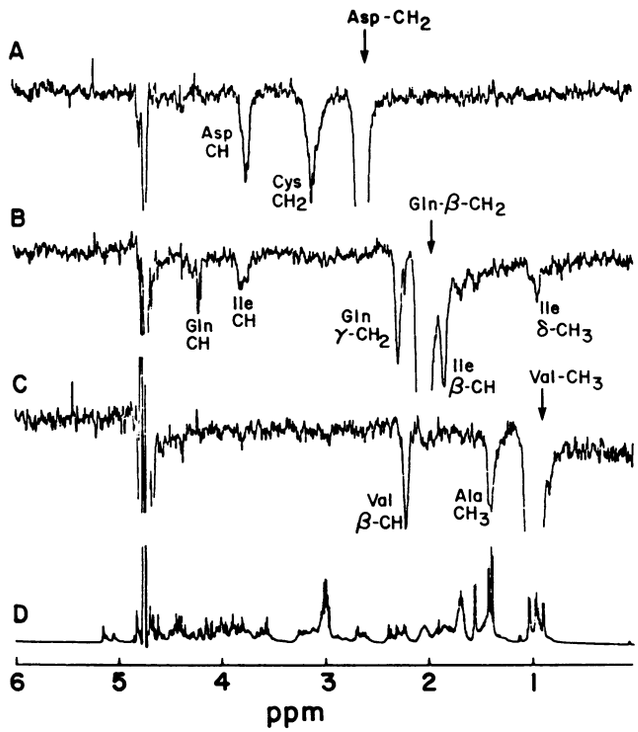

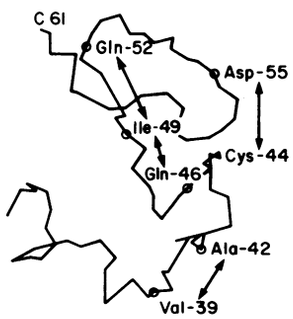

FIG. 3. (*A–C*) ^1H–^1H NOE difference spectra (500 MHz) of the α_{II} fragment (4 mM) in ^2H_2O at 30°C. The arrows indicate the position of the irradiation frequency. The assignment of the resonances is indicated below the spectra and the positions of the corresponding amino acids in the molecule are shown on the computer graphics to the right, where all carbon and nitrogen atoms of the chain are represented. (*D*) Normal ^1H NMR spectrum acquired under the same conditions.

the methylene resonances of aspartate-55 were irradiated (Fig. 3A), a NOE was observed for the CH_2 protons of a cysteine residue. Based on our molecular model, cysteine-44, one of the cysteine residues coordinated to Cd_5, is located in close proximity to aspartate-55. It is interesting to note the correspondence between this ^1H NOE data and the observation of two ^{113}Cd resonances for Cd_5 of human liver MT-1 originating from the heterogeneity at position 55, as discussed earlier.

In another ^1H–^1H NOE experiment, the β-CH_2 protons of a glutamine residue(s) (Fig. 3B) were irradiated. In this case, a NOE was observed for the ^1H resonances of isoleucine-49 (a unique residue) indicating its proximity to a glutamine residue. The two glutamine residues† of the α_{II} fragment from rat liver are expected to be located at positions 46 and 52 based on the sequence homology with mouse liver MT-2 (16, 17). Due to the overlapping β-CH_2 resonance of the two glutamines, we could not selectively irradiate the protons of a single residue. However, both glutamine-46 and glutamine-52 are in close proximity to isoleucine-49 in our model and could give rise to a NOE. Additional ^1H–^1H NOE experiments indicated that valine-39 is in the environment of an alanine residue (Fig. 3C). Based on our model, only one of the three alanine residues that are present in the primary sequence, alanine-45, is found in close enough proximity to valine-39 for a dipolar interaction. All of the NOE data obtained for the MT fragment were consistent with the structure of our proposed model.

Conclusion

On the basis of a consideration of all the physicochemical, and in particular the NMR data, it has been possible to derive a molecular model of MT. The unique disposition of the cysteines along the chain limits the number of possible structures for the protein, in particular for the 4-metal cluster portion where the availability of the α fragment has enabled us to verify several of our structural predictions by ^1H NMR.

This study provides an excellent illustration of the potential of the NMR technique for the determination of structure of a small protein that continues to defy crystallization. Although the predicted structure of MT is not unique, a combination of ^1H and ^{113}Cd NMR has provided insight into its major structural features, especially relating to the two-domain structure, each domain containing a distinct metal cluster. If and when an x-ray structure becomes available, some refinement to our model will undoubtedly be necessary; however, we believe it unlikely that these corrections will represent sufficiently significant excursions from the structure presented herein to negate its use in our continued efforts to elucidate the biological function(s) of MTs.

The authors thank Barry Levinson for running the Chou–Fasman computer program, Dr. K. R. Williams for the α-fragment sequence determination, and Mark Handschumacher for his assistance in the use of the computer graphics to model the protein. The α_{II} rat MT sample used in this study was kindly provided by Dr. D. R. Winge. The financial assistance of National Institutes of Health Grant AM 18778, National Science Foundation Grant CHE-7916210, and a North Atlantic Treaty Organization Postdoctoral Fellowship (Y.B.) is also gratefully acknowledged.

1. Margoshes, M. & Vallee, B. L. (1957) *J. Am. Chem. Soc.* **79**, 4813–4814.
2. Nordberg, M. & Kojima, Y. (1979) in *Metallothionein*, eds. Kägi, J. H. R. & Nordberg, M. (Birkhäuser, Basel, Switzerland), pp. 41–117.
3. Kägi, J. H. R. & Vallee, B. L. (1961) *J. Biol. Chem.* **236**, 2435–2442.
4. Vallee, B. L. (1979) in *Metallothionein*, eds. Kägi, J. H. R. & Nordberg, M. (Birkhäuser, Basel, Switzerland), pp. 19–40.
5. Squibb, K. S., Cousins, R. J. & Feldman, S. L. (1977) *Biochem. J.* **164**, 223–228.
6. Ohi, S., Cardenosa, G., Pine, R. & Huang, P. C. (1981) *J. Biol. Chem.* **256**, 2180–2184.
7. Cherian, M. G. & Goyer, R. (1978) *Life Sci.* **23**, 1–10.
8. Johnson, D. R. & Foulkes, E. C. (1980) *Environ. Res.* **21**, 360–365.
9. Winge, D. R., Premakumar, R. & Rajagopalan, K. V. (1975) *Arch. Biochem. Biophys.* **170**, 242–252.
10. Suzuki, K. T. & Yamamura, M. (1980) *Biochem. Pharmacol.* **29**, 2407–2412.
11. Otvos, J. D. & Armitage, I. M. (1979) *J. Am. Chem. Soc.* **101**, 7734–7736.
12. Otvos, J. D. & Armitage, I. M. (1980) *Proc. Natl. Acad. Sci. USA* **77**, 7094–7098.
13. Briggs, R. W. & Armitage, I. M. (1982) *J. Biol. Chem.* **257**, 1259–1262.
14. Boulanger, Y. & Armitage, I. M. (1982) *J. Inorg. Biochem.* **17**, 147–153.
15. Armitage, I. M., Otvos, J. D., Briggs, R. W. & Boulanger, Y. (1982) *Fed. Proc. Fed. Am. Soc. Exp. Biol.* **41**, 68–74.
16. Huang, I.-Y., Yoshida, A., Tsunoo, H. & Nakajima, H. (1977) *J. Biol. Chem.* **252**, 8217–8221.
17. Huang, I.-Y., Kimura, M., Hata, A., Tsunoo, H. & Yoshida, A. (1981) *J. Biochem.* **89**, 1839–1845.
18. Kimura, M., Otaki, N. & Imano, M. (1979) in *Metallothionein*, eds. Kägi, J. H. R. & Nordberg, M. (Birkhäuser, Basel, Switzerland), pp. 163–168.
19. Kissling, M. M. & Kägi, J. H. R. (1979) in *Metallothionein*, eds. Kägi, J. H. R. & Nordberg, M. (Birkhäuser, Basel, Switzerland), pp. 145–152.
20. Kissling, M. M. & Kägi, J. H. R. (1977) *FEBS Lett.* **82**, 247–250.
21. Kojima, Y. & Kägi, J. H. R. (1978) *Trends Biochem. Sci.* **1**, 90–93.
22. Kojima, Y., Berger, C. & Kägi, J. H. R. (1979) in *Metallothionein*, eds. Kägi, J. H. R. & Nordberg, M. (Birkhäuser, Basel, Switzerland), pp. 153–161.
23. Kojima, Y., Berger, C., Vallee, B. L. & Kägi, J. H. R. (1976) *Proc. Natl. Acad. Sci. USA* **73**, 3413–3417.
24. Lerch, K., Ammer, D. & Olafson, R. W. (1981) *FEBS Lett.* **126**, 165–168.
25. Lerch, K. (1979) in *Metallothionein*, eds. Kägi, J. H. R. & Nordberg, M. (Birkhäuser, Basel, Switzerland), pp. 173–179.
26. Bühler, R. H. O. & Kägi, J. H. R. (1979) in *Metallothionein*, eds. Kägi, J. H. R. & Nordberg, M. (Birkhäuser, Basel, Switzerland), pp. 211–220.
27. Weser, U. & Rupp, H. (1979) in *Metallothionein*, eds. Kägi, J. H. R. & Nordberg, M. (Birkhäuser, Basel, Switzerland), pp. 221–230.
28. Rupp, H. & Weser, U. (1978) *Biochim. Biophys. Acta* **533**, 209–226.
29. Vašák, M., Kägi, J. H. R. & Hill, H. A. O. (1981) *Biochemistry* **20**, 2852–2856.
30. Durnam, D. M., Perrin, F., Gannon, F. & Palmiter, R. D. (1980) *Proc. Natl. Acad. Sci. USA* **77**, 6511–6515.
31. Glanville, N., Durnam, D. M. & Palmiter, R. D. (1981) *Nature (London)* **292**, 267–269.
32. Karin, M. & Richards, R. I. (1982) *Nature (London)* **299**, 797–802.
33. Winge, D. R. & Miklossy, K.-A. (1982) *J. Biol. Chem.* **257**, 3471–3476.
34. Boulanger, Y., Armitage, I. M., Miklossy, K.-A. & Winge, D. R. (1982) *J. Biol. Chem.* **257**, 13717–13719.
35. Kägi, J. H. R., Himmelnoch, S. R., Whanger, P. D., Bethune, J. L. & Vallee, B. L. (1974) *J. Biol. Chem.* **249**, 3537–3542.
36. Fiskin, A. M., Peterson, G. & Brady, F. O. (1977) *Ultramicroscopy* **2**, 389–395.
37. Hennessey, J. P., Jr., & Johnson, W. C., Jr. (1981) *Biochemistry* **20**, 1085–1094.
38. Fasman, G. D. (1980) *Ann. N.Y. Acad. Sci.* **348**, 147–159.
39. Murphy, P. D., Stevens, W. C., Cheung, T. T. P., Lacelle, S., Gerstein, B. C. & Kurtz, D. M., Jr. (1981) *J. Am. Chem. Soc.* **103**, 4400–4405.
40. Gilbert, W. (1978) *Nature (London)* **271**, 501.
41. Vašák, M., Galdes, A., Hill, H. A. O., Kägi, J. H. R., Bremner, I. & Young, B. W. (1980) *Biochemistry* **19**, 416–425.